AUT Journal of Civil Engineering

AUT J. Civil Eng., 3(1) (2019) 93-106
DOI: 10.22060/ajce.2018.14763.5496

Experimental Investigation of Steel-concrete-steel Slabs with Stud Bolt Connectors Subjected to Punching Loading

M. Golmohammadi[1*], M. Ghalehnovi[2], M. Yousefi[3]

[1] Civil Engineering Department, Faculty of Engineering, University of Torbat Heydarieh, Torbat Heydarieh, Iran
[2] Civil Engineering Department, Faculty of Engineering, Ferdowsi University of Mashhad, Mashhad, Iran
[3] Civil Engineering Department, Faculty of Maritime Engineering, Chabahar Maritime University, Chabahar, Iran

ABSTRACT: Steel-Concrete-Steel (SCS) sandwich structures are composed of two steel face plates and one concrete core. SCS as slab has more advantages than reinforced concrete (RC) slab that their most important are impermeability and higher resistance against impact loads. SCS sandwich slabs are widely employed in civil engineering and onshore and offshore structures due to their better performance and advantages. Mechanical connectors are used for better performance of the slabs. In the present research, stud bolt connectors are used together with nuts. The core is composed of ordinary concrete. Nine test samples of SCS slabs are made with stud bolt connectors and are put under concentrated load at the center of the slab. The observed failure modes included concrete core crack, lower plate slip and upper plate buckling, and stud bolt separation. To study load vs. displacement at the center and load vs. interlayer slip behavior, stud bolts diameter and concrete thickness were varied. The results of the tests were compared with the results of sandwich slabs with J-hook connectors and a better behavior was observed. One theoretical model was used to predict the bending strength of the slabs. The results of the theoretical model were consistent with test results.

Review History:
Received: 29 July 2018
Revised: 2 October 2018
Accepted: 2 October 2018
Available Online: 18 October 2018

Keywords:
Bending Strength
Double-sided Cutting
Failure Modes
SCS Sandwich Slab
Stud Bolt Connector

1- Introduction

SCS sandwich structure is a rather new structure dating back to 1970s [1]. This structure benefits the advantages of compressive strength of concrete and tensile strength of steel. SCS sandwich structure has more advantages than reinforced concrete (RC) structure. Some of its advantages include removal of concrete formwork, prefabricated application, cost reduction and shorter construction period, impermeability, higher resistance against scaling under impact loads, and easier repair. SCS sandwich structures are widely employed in civil engineering and onshore and offshore structures due to their better performance and advantages [2-6].

On the other hand, due to suitable concrete confinement by metal plates, suitable behavior is expected against impact and burst. It provides advantages beyond pre-stressed concrete or steel in terms of safety, serviceability, toughness, economy and easy fabrication [7].

Since SCS system is applied in three layers, its performance cannot be considered as an integrated composite, and large cracks develop in the concrete core. Although the type of connectors and their arrangement influence the control of concrete cracking due to the decrease in interlayer slip, the slip occurs eventually and even very small slips lead to concrete cracking. The important issue is to reduce the cracks as much as possible [8-10].

Also, through type design, very suitable elements can be created to be manufactured in factory in units that require the lowest on-site welding for assembling the members [11].

One way to connect the plates to the concrete is to use epoxy adhesive that does not show good resistance against interlayer slip. To improve SCS sandwich behavior, different shear connectors are suggested as mechanical connectors and some of them are applied. Overlapped stud bolt shear connectors have been the first type of the shear connectors (Figure 1a). In this system, stud bolt shear connectors are welded to the skin at one end, and double skin connection is provided by concreting and burying the other end of shear connectors in the concrete [12-17]. Bi-steel connectors are another type of shear connectors (Figure 1b). In this structure, external face plates are connected by rod connectors with friction welding. As a result, tensile separation is prevented [8, 18-22].

Another type of SCS sandwich connectors are J-hook connectors (Figure 1c). This type of shear connectors are interlocked as pairs and are welded to two steel face plates to transfer interlayer shear forces, resist tensile separation and prevent from local buckling of steel face plates [23-32].

Corresponding author, E-mail: m.golmohammadi@torbath.ac.ir

In addition, other shear connectors are suggested to be used in SCS sandwich structure that are indicated in Figures 1d-e and are applied less. Also, for corrugated strip connectors innovated by Leekitwattana et al. there is welding limitation to be welded at both ends (see Figure 1f). However, Yousefi and Ghalehnovi presented experimental and numerical investigations of these connectors as one end welded in SCS structure. The simple construction of these shear connectors with steel plate and bending is the main advantage of them. Concrete cracking along the legs of these connectors was the most important disadvantage of them because one end is buried in concrete without being welded to the opposite side (see Figure 1g) [33, 34].

(c) J-hook connectors [35]

(b) Bi-steel connectors [19]

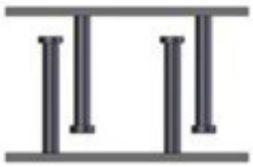

(a) Overlapped stud bolt connectors [12]

(f) Corrugated-strip connectors [38]

(e) Channel connectors [37]

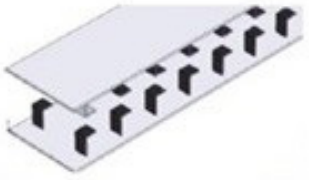

(d) Angle connectors [36]

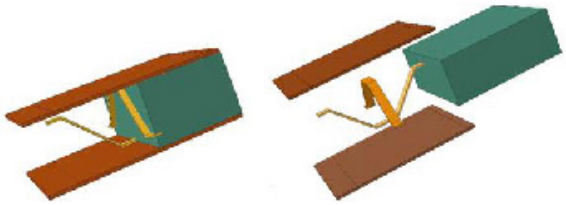

(g) One end welded corrugated-strip connectors [33, 34]

Figure 1. Different types of shear connectors

One of the other shear connectors that has been studied less in earlier researches is stud bolt shear connector (see Figure 2). These connectors are easily accessible and are applied easily in construction sites. On the other hand, they provide full connection between two plates without any limitation in the thickness between two face plates. In the present research, the behavior of such these connectors is examined in SCS sandwich slabs. As Figure 3, SCS sandwich slab with stud bolt shear connectors is one of the important applications of such these materials. Golmohammadi and Ghalehnovi (2018) investigated interlayer shear behavior of stud bolts [39].To investigate the effect of parameters on interlayer shear behavior of steel-concrete-steel sandwich structure with stud bolt connectors, push-out test was performed under progressive loading. In the present research, nine SCS sandwich slabs with stud bolt shear connectors and simple supports are studied and tested under Gradual incremental loading as flexural and punching shear force. Then failure modes of the slabs, load-displacement and load-slip curves are discussed. Finally, the results of the tests are compared with the results of sandwich slabs with J-hook connectors. Also, one theoretical model is suggested to predict the bending strength of the slabs. In this study, the effects of the shocks, system rigidity, vibration and lateral loading of the slab are ignored and can be the future program of the team especially under impact and dynamic loading.

Figure 2. Stud bolt shear connector

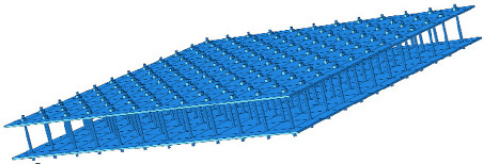

Figure 3. SCS sandwich slab configuration with stud bolt connectors

2- Test program

To study the static performance of SCS sandwich slabs with stud bolt shear connectors, a test is performed by applying static load using a block concentrated at the center of slab. In the test, the following variables are taken into account: concrete core thickness (80, 100 and 150 mm), stud bolt diameter (8, 10, 12 mm) and stud bolts' spacing (80, 100, 150 mm).

Nine test samples of SCS sandwich slabs were prepared with the dimensions 1200 ×1200 mm^2. SCS slabs with stud bolt connectors are named as "SCSB" briefly. Following SCSB, the diameter of the stud bolt connector is presented in mm. From any slab with a certain stud bolt diameter, three samples are prepared with different core thicknesses. In Table 1, geometrical specifications of the samples are presented.

Steel plates were cut in the factory with the selected dimensions and the location of stud bolts were pierced by CNC machine. Finally, stud bolts and nuts were put in their position with a certain distance.

As stud bolts and nuts were fixed in their position, test samples were prepared for concreting. Since concreting must be performed vertically, both sides of samples were moulded and all samples were controlled by a belt to prevent from their dislocation. Concreting of samples was performed concurrently and cylindrical samples were prepared for compressive and tensile strength test of concrete. The stages are shown in Figure 4.

(a) assembling plates and stud bolts

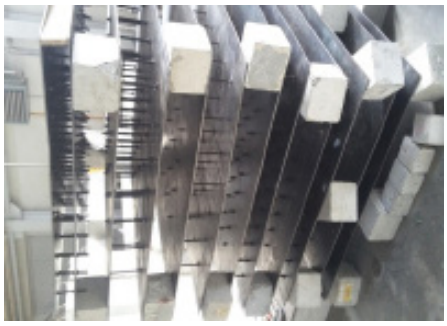

(b) slabs prepared before concreting

(c) installing the moulds and setting up the slabs vertically for concreting

(d) SCS sandwich slab with stud bolt connectors

Figure 4. Stages of SCS sandwich slab preparation with stud bolt connectors

Table 1. Geometrical specifications of SCSB test samples

No.	Sample	Dimensions of plate (mm^3)	Concrete thickness (mm)	Stud bolt diameter (mm)	Stud bolts' spacing (mm)	Number of holes
1	SCSB8-1	1200×1200×6	80	8	100	121
2	SCSB8-2	1200×1200×6	100	8	100	121
3	SCSB8-3	1200×1200×6	150	8	150	49
4	SCSB10-1	1200×1200×6	80	10	100	121
5	SCSB10-2	1200×1200×6	100	10	100	121
6	SCSB10-3	1200×1200×6	150	10	150	49
7	SCSB12-1	1200×1200×6	80	12	100	121
8	SCSB12-2	1200×1200×6	100	12	100	121

3- Properties of materials

As slabs were concreted, the concrete was sampled to test the compressive and tensile strengths. The test results of compressive and tensile strengths of concrete are given in Tables 2 and 3 for 28-days cylindrical samples.

To obtain mechanical properties of steel face plates, standard dog-bone shaped samples were prepared and were put under tension. Dog-bone shaped samples are prepared according to ASTM E8M Standard. Standard samples were also prepared from stud bolts and were put under direct tension. After drawing engineering plastic stress-strain curves and actual plastic stress-strain curves for plates and stud bolts, mechanical properties of the materials are summarized in Tables 4 and 5.

Table 2. Compressive strength of cylindrical samples

Sample's age (days)	Compressive strength of samples (f_{sp}) (Mpa)	Average compressive strength of samples (f_c) (Mpa)	Standard deviation	Dispersion coefficient
28	38.6	38.5	0.70	0.018
	39.2			
	37.8			

Table 3. Tensile strength of cleavage test of cylindrical samples

Sample's age (days)	Tensile strength of samples (f_{sp}) (Mpa)	Average tensile strength of samples(f_c) (Mpa)	Standard deviation	Dispersion coefficient
28	3.70	3.75	0.05	0.013
	3.76			
	3.80			

Table 4. Mechanical properties of steel plates from direct tension test

Thickness (mm)	E_s (Gpa)	Yield stress (MPa)	Ultimate stress (MPa)	Strain in ultimate stress
6	205	323	560	0.23

Table 5. Properties of stud bolts from direct tension test

Stud bolt diameter (mm)	E_s (Gpa)	Yield stress (MPa)	Ultimate stress (MPa)	Strain in ultimate stress
8	217	745	890	0.061
10	205	764	867	0.058
12	207	730	908	0.057

4- Test instruments

28 days after concreting, the slabs must be transferred to the loading place. In this period, samples were kept wet to be processed. Two hooks were welded to both sides of slabs and were moved by a crane. Weight of slabs ranged from 450 to 700 kg. Their relocation and alignment in the loading place needs a lot of care. Set up of test instruments of SCSB sandwich slabs under concentrated load is indicated in Figure 5. The slab is put on simple supports at four sides (Figure 5a) and the concentrated load is applied by a hydraulic jack at the center of the slab under displacement mode control (see Figure 5b).

The slab is put on continuous supports at four sides and the distance of the supports from the slab's edges is 100 mm. Thus, the effective span of the slab is 1000 mm in any direction. The concentrated load is applied at the center of the sample with the dimensions 100 ×100 mm^2.

The applied load is measured using a calibrated load cell put under the loading jack (see Figure 5b). As Figure 5c, displacement of the slab's center is obtained by a laser LVDT installed under the slab. Also, the slip between the lower steel plate and concrete in the sample's edge is obtained from the difference between values of LVDTs installed on the lower steel plate and the adjacent concrete (see Figure 5d). The concrete core is painted white to show the cracks on the concrete during the test.

LVDTs and load cells are connected to a computer and register data during the test. Load against displacement is registered simultaneously until the samples fail. Loads related to the concrete's cracks are observed and marked on the concrete.

(a) Simple support

(b) Putting the sample on the support and loading by a rigid component

(c) Installation of LVDT in the central point under the sample

(d) Installation of LVDT on the edge of concrete and steel plate

Figure 5. Set up of test instruments

5- Test results and observations

In this section, failure modes of slabs and load-displacement and load-slip curves are investigated.

5- 1- Behavior of test samples

Behavior of all slabs is identical in the first stage of loading. In the first step, load increases with tension cracks in the concrete core that is expected. In the second step, as the lower plate slips and the upper plate buckles, one or more connectors are likely to fail. When the natural bonding between steel plates and concrete core fails, connectors resist shear forces. The internal cracks of the concrete core were not observable, because they were between steel plates. Although the cracks on the concrete surface were observed around the slabs in the test and were marked as load increased and cracks developed, slip occurred as the load increased between the concrete and lower plate, and sometimes, the plate separated from the concrete at the edges. Also, those regions around the loading environment have penetrated into the concrete. As load increased more, the upper plate buckled. As load increased and the slip between the lower plate and concrete increased, stud bolts separated from the plate and sounds were produced. Stud bolts separation starts from the outer edge of the plate and gradually, it proceeds to the center of the slab. When the separation of stud bolts was large, the lower plate separated from the concrete.

To observe concrete core behavior, autopsy is performed after sample unloading. In fact, upper bolts and nuts are opened by a wrench and the upper plate is removed from the bolts. Thus, the surface of the concrete core and pattern of cracks are observed.

For example, development of cracks and failure modes of SCSB10-3 slab are shown in Figure 6.

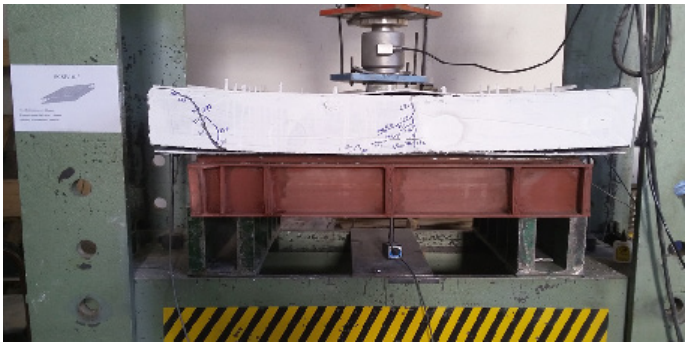

(a) loading and development of cracks in SCSB10-3 slab

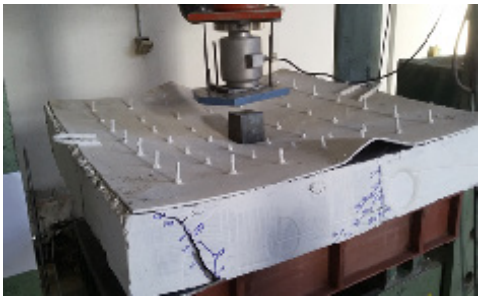

(b) buckling of upper plate at the center of the adjacent side of the slab

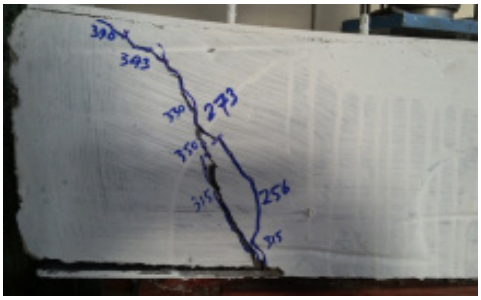

(c) shear crack of concrete and separation of lower plate from concrete

(d) removal of upper plate and observation of cracks on the concrete surface

(e) development of internal cracks of the concrete to the external surface of slab

Figure 6. Failure modes of SCSB10-3 slab

5- 2- Load-displacement curves

Load-displacement curves of the slab's center are drawn for SCSB slab test samples under the effect of the concentrated load. Generally, as load increased, displacement of the slab's center increased and samples showed a good ductility. As the concentrated load increased, stiffness decreased that was tangent to the load-displacement curve. In this section, the effect of different parameters is examined on load-displacement curves.

5- 2- 1- Effect of stud bolt diameter

Pattern of cracks development is shown for the samples SCSB8-3, SCSB10-3 and SCSB12-3 in Figure 7. According to the figure, cracks are flexural in SCSB8-3 sample with a lower stud bolt diameter. However, as stud bolt diameter increases in SCSB10-3 and SCSB12-3 samples, number of cracks increases and they emerge as flexure-shear cracks.

In Figure 8, the effect of different stud bolt diameters is shown by load-displacement curves. As it is observed, as stud bolt diameter increases, more force is required for a constant displacement, showing the direct relation between stud bolt diameter and SCSB slab strength. This increase in strength is shown in Figure 8a with a concrete thickness of 80 mm and a stud bolts' spacing of 100 mm and a constant displacement of 51 mm. According to the figure, relative to the stud bolt diameter of 8 mm (SCSB8-1 specimen), the strength is increased by 14% for 10 mm (SCSB10-1 specimen) and about 27% for a diameter of 12 mm (SCSB12-1 specimen). For specimens of Figure 8b with a concrete thickness of 100 mm and a stud bolts' spacing of 100 mm and a constant displacement of 47 mm, relative to the stud bolt diameter of 8mm (SCSB8-2), the strength is increased by 30% for a diameter of 10mm (SCSB10- 2 specimen) and about 70% for a diameter of 12 mm (SCSB12-2 specimen). In Figure 8c and the SCSB8-3 specimen, despite increasing the thickness of the concrete to 150 mm, due to the increase in the stud bolts' spacing to 150 mm and the weak stud bolts of the 8 mm, the stiffness and the strength of the slab are noticeably reduced. In each case, the strength increased by 30% as the stud bolt increased to 10 mm (SCSB10-3 specimen). However, with a diameter of 12 mm (SCSB12-3 specimen), a considerable improvement in stiffness and strength is achieved, so that the strength is almost doubled.

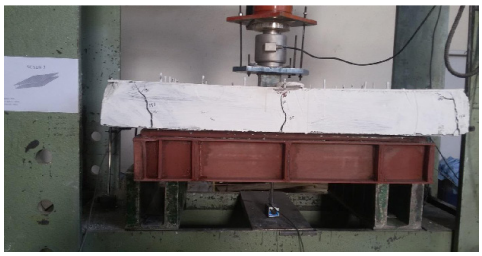

(a) Cracks development in SCSB8-3 sample

(b) Cracks development in SCSB10-3 sample

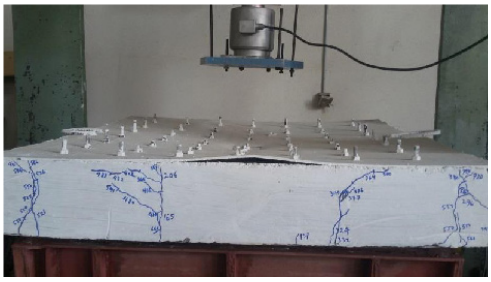

(c) Cracks development in SCSB12-3 sample

Figure 7. Comparison of cracks development in slabs with different stud bolt diameters

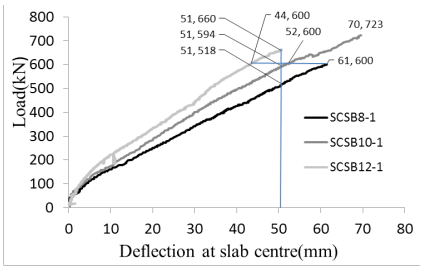

(a) The concrete thickness 80 mm and with stud bolts' spacing 100 mm

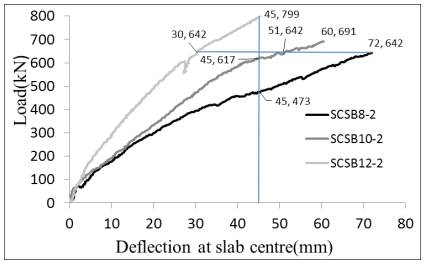

(b) The concrete thickness 100 mm and with stud bolts' spacing 100 mm

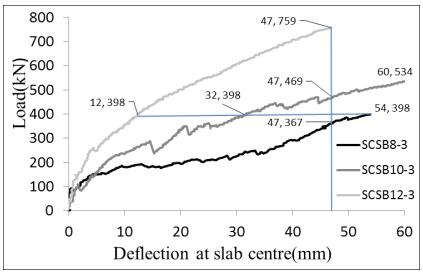

(c) The concrete thickness 150 mm and with stud bolts' spacing 150 mm

Figure 8. Comparison of samples with different stud bolt diameters

5- 2- 2- Effect of concrete thickness

It is observed in Figure 9 that as concrete core thickness increases, pattern of cracks development changes from flexural crack to flexure-shear crack.

Also, strength and stiffness of samples increased due to the increase in concrete core thickness as in Figure 10. The increase in strength continues until the concrete reaches its ultimate strength. Afterwards, strengths of samples become close to each other. As concrete core thickness increases, energy absorption (area under the curve) increases.

According to Table 6, failure modes are normally less in samples with a lower thickness than those with a higher thickness. For example, SCSB8-1 sample has the concrete thickness 80 mm and SCSB8-2 sample has the concrete thickness 100 mm. Failure modes of the sample SCSB8-1 include only lower plate slip and one stud bolt separation. However in SCSB8-2 sample, there are more than 10 separations of stud bolts and a slight upper plate buckling in addition to the lower plate slip. It is observed that the strength of the sample SCSB8-2 is higher and it has more failure modes. The reason is that for higher core strength, there must be a stronger stud bolt but its stud bolt strength is similar to the sample SCSB8-1. Therefore, the steel parts fail more.

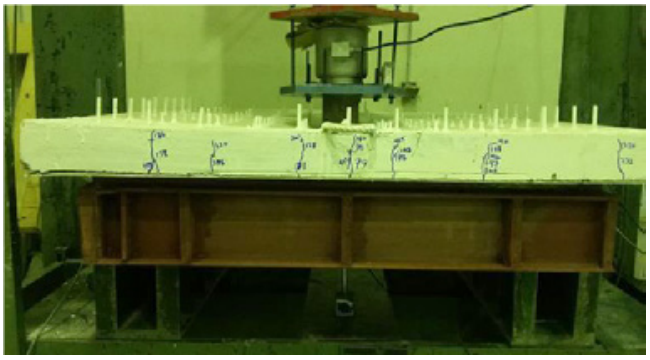

(a) Cracks development in SCSB8-1 sample

(b) Cracks development in SCSB8-2 sample

Figure 9. Comparison of cracks development in slabs with different concrete core thicknesses

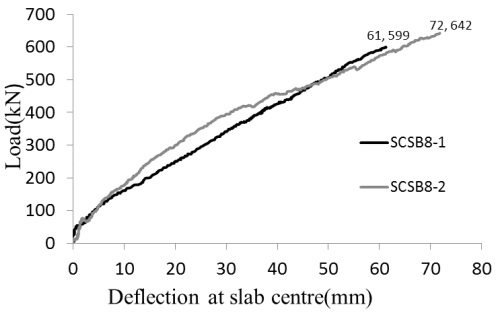

(a) With the stud bolt diameter 8 mm

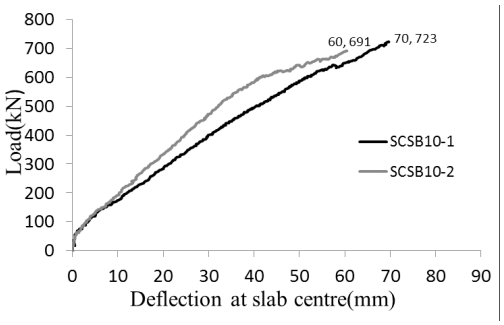

(b) With the stud bolt diameter 10 mm

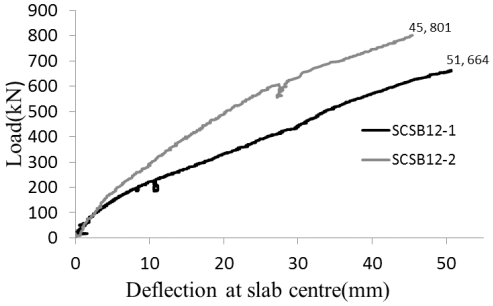

(c) With the stud bolt diameter 12 mm

Figure 10. Effect of concrete thickness on SCSB slab strength

Table 6. Failure modes

Sample	Lower plate slip	Stud bolt separation	Upper plate buckling
SCSB8-1	Yes	One case	No
SCSB8-2	Yes	More than 10 cases	Slight
SCSB10-1	Yes	More than 10 cases	No
SCSB10-2	Yes	More than 10 cases	No
SCSB12-1	No	No	No
SCSB12-2	Yes	No	No

5- 3- Comparison of load displacement curve with earlier research

Sohel and Liew [25] studied the behavior of SCS slabs with J-hook connectors by performing tests. In this test program, SCS slabs were studied with lightweight concrete, ordinary concrete and fiber concrete. Dimensions of test samples and loading conditions were similar to the present research. In the above research, SCS6-100 sample has geometrical specifications similar to SCSB10-2 in the present research. In both samples, concrete core thickness is 100 mm, spacing of connectors is 100 mm, diameter of connectors is 10 mm, plate thickness is 6 mm and the concrete is ordinary. The only difference between both samples is the type of connectors. In SCS6-100 slab, a pair of J-hook connectors is used with the diameter 10 mm and σ_y= 315 (MPa) . However in SCSB10-2 slab, stud bolt connectors are used with the diameter 10 mm and σ_y= 725 (MPa) and nuts are used to provide connection to steel plates.

Figure 11 shows load-displacement curves of two slabs. In load-displacement curve of SCS6-100 slab, after the first peak, load declines rapidly. The load decline shows that the shear capacity of both sides of the concrete core dominates the bending capacity. After the load declines, it increases again and the membrane performance of the steel plate occurs. However in SCSB10-2 slab, as the load increases, displacement also increases and better ductile behavior and composite performance are observed. In fact, better connection of plates by stud bolts makes the concrete more confined and the concrete strength is exploited to increase the slab strength. In this slab, the bending capacity dominates the shear capacity at both sides.

Displacement of SCS6-100 slab's center is 7.29 mm in the maximum load 620.93 kN. However, displacement of SCSB10-2 slab's center is 45.11 mm for the same load, showing higher energy absorption. The above advantages together with easier application of stud bolt connectors in construction sites show the relative superiority of this type of connectors compared to J-hook connectors.

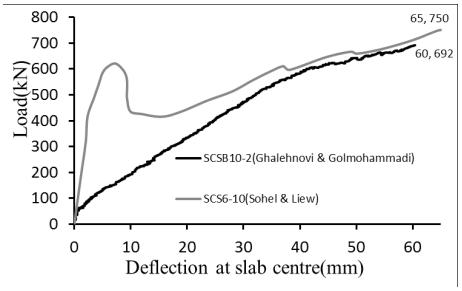

Figure 11. Comparison of load-displacement curve of a slab with J-hook and stud bolt connectors

6- Push-out test for extracting the shear strength of the stud bolt

To calculate the analytical value of the bending capacity (F_p) of the slab under punching loading, before anything interlayer shear capacity (P_R) of the slabs must be obtained. For this purpose, Golmohammadi and Ghalehnovi (2018) as Figure 12 studied SCS samples with ordinary concrete core and stud bolt connectors under push-out test [39]. Authors performed push-out test on 16 test samples under quasi-static loading. Generally, important parameters affecting interlayer shear strength of SCS sandwich structures with stud bolt connectors include geometrical specifications of the system and mechanical properties of materials including steel, concrete and stud bolt.

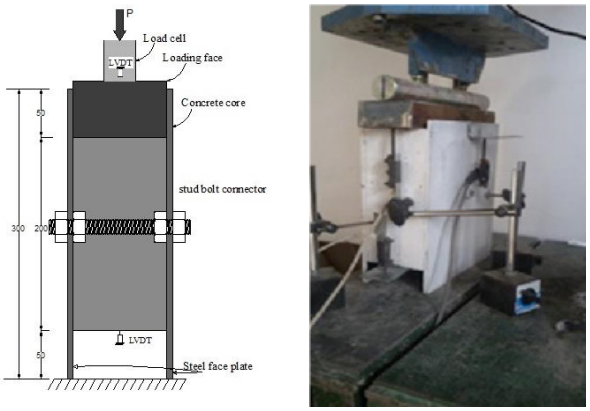

Figure 12. Instruments of push-out test [39]

The numerical model of the push-out test is presented on one main component of SCS sandwich structure with stud bolt shear connectors. To verify the modeling results, push-out test is performed using the test samples under quasi-static loading. ABAQUS/Explicit Solver is used due to the geometric complexity of the finite element model.

In order to simulate quasi-static loading in Explicit Analysis properly, kinetic energy was not allowed to exceed 5% to 10% of the internal energy. Also, to verify the modeling results, shear force-slip curve, ultimate shear strength and failure modes were compared with test results. The results showed that finite element model using mass scaling in Explicit Solver agrees acceptably with the test results with a suitable analysis speed.

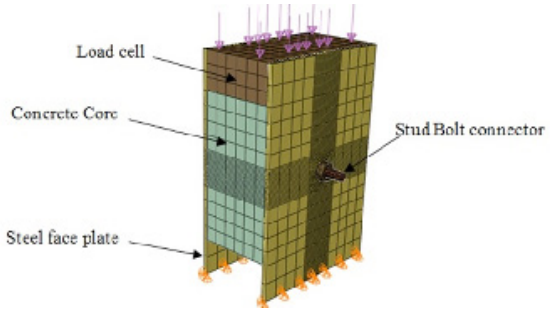

Figure 13. Finite element model of push-out test [39]

Using the regression analysis on the results of 80 numerical models of push-out test, a relation was obtained to calculate the ultimate shear strength per unit area (P_R/A_s). Variables affecting the ultimate shear strength include steel face plates thickness, t_p, concrete compressive strength, f_c, and concrete core thickness to shear connectors diameter, h_c/d. The relation 1 was proposed for the failure mode of the concrete [39]:

$$\frac{P_R}{A_S} = 0.047 t_p^{0.22} f_c^{0.3} \left(\frac{h_c}{d}\right)^{0.46} \quad (1)$$

The results of the proposed relation are used to predict the ultimate shear strength of stud bolt connectors.

7- Analytical relation of the bending capacity of SCS sandwich slab

In SCS sandwich slabs, bending capacity can be evaluated using the yield line theory Figure 14 shows the failure pattern of yield lines in a square slab with simple supports at four sides, with the slab's center being under concentrated load. According to virtual work principle, the bending capacity of the slab can be obtained using the relation proposed by Rankin and Long [40] as follows:

$$F_p = 8 m_{pl} \left(\frac{L_S}{L-c} - 0.172\right) \quad (2)$$

Where:

m_{pl} = plastic bending capacity per unit length along the yield line

c= length of loading rigid component's side

L_s= dimensions of slab test sample

L= span length between supports

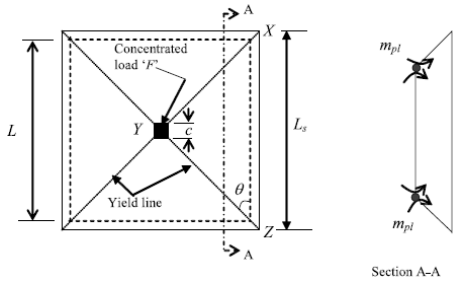

Figure 14. Mechanism of the yield line of the sandwich slab under concentrated load at the center of slab [41]

Plastic moment of resistance of a complete SCS sandwich section can be obtained by assuming a rectangular block of plastic stress with width b and depth x_c for the concrete (Figure 15). It is assumed that the concrete is cracked under the plastic neutral axis (PNA). Forces of steel plates depend on the yield strength of materials and shear strength of connectors between concrete core and steel plate border. It is also assumed that sufficient shear connectors are supplied to prevent from the local buckling of the compressive steel plate.

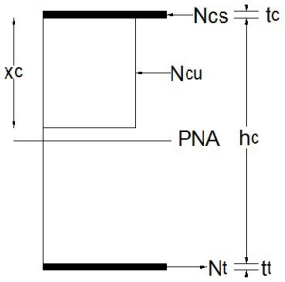

Figure 15. Force distribution in the section in complete plastic stage

The compression force of the concrete (N_{cu}) is given by Eurocode4 [42] as follows:

$$N_{cu} = \frac{0.85 f_c}{\gamma_c} b x_c \quad (3)$$

osition of plastic neutral axis can be obtained by equalizing tensile and compression forces:

$$N_{cs} + N_{cu} = N_t \quad (4)$$

Substituting $N_{cs}=\sigma_y b t_c$, $N_t=\sigma_y b t_t$ and N_{cu} from the relation 3 in the relation 4, depth of stress block is obtained by the following relation:

$$x_c = 1.176 \gamma_c \sigma_y (t_t - t_c) / f_c \quad (5)$$

Where γ_c= 1.5 is a partial factor of the concrete proposed by Eurocode [43]. Taking the moment relative to the center of the compressive steel plate, the plastic moment of the resistance of the sandwich section is obtained:

$$M_{pl} = \sigma_y b t_t (h_c + \frac{t_c}{2} + \frac{t_t}{2}) - \frac{0.85 f_c b x_c}{\gamma_c}(0.5x_c + \frac{t_c}{2}) \quad (6)$$

If the thickness of upper and lower plates are equal $t_c = t_t$, it is expected that SCS sandwich section fails as a brittle state. SCS sandwich slab will normally bend and the sides of cracks at the concrete core will develop in final loading stages. After tensile steel plate yielding, cracks of the concrete core continue toward the upper compressive plate. The section reaches its ultimate bending capacity if the neutral axis moves toward the lower surface of the compressive steel plate ($x_c \approx 0$) and the upper steel plate yields eventually. Therefore, if $t_c = t_t = t$, plastic moment of resistance of sandwich section is obtained from the relations 5 and 6 as follows:

$$M_{ult} = \sigma_y b t (h_c + t) \quad (7)$$

The relation 7 does not consider the tensile failure of the lower plate. Therefore, the tensile strain of the lower plate must not exceed the final strain.

If the longitudinal tensile force (N_t) and the compression force (N_{cs}) of the steel plate are controlled by the shear connector capacity, SCS structure is called "partial composite" and the relation 3 is written as follows:

$$N_{cs} + 0.85 f_c b x_c / \gamma_c = N_t \quad (8)$$

Or

$$x_c = 1.176 \gamma_c (N_t - N_{cs}) / f_c b \quad (9)$$

If the number of shear connectors decreases, the moment of resistance of the partial composite structure decreases too. Taking the moment around the center of the compressive steel plate, the plastic moment of resistance of the partial composite section can be determined by the following relation:

$$M_{pl} = N_t (h_c + \frac{t_c}{2} + \frac{t_t}{2}) - \frac{0.85 f_c b x_c}{\gamma_c}(0.5x_c + \frac{t_c}{2}) \quad (10)$$

where $N_t = n_p P_R$. Normally, the number of stud bolt connectors is equal in upper and lower plates. If both sides of plates have similar thickness and strength, x_c is zero. Assume that $t_c = t_t = t$ and $N_t = n_p P_R$, the relation 10 is summarized as follows:

$$M_{pl} = n_p P_R (h_c + t) \quad (11)$$

Now, consider a square SCS slab including n_t stud bolt shear connectors connected to upper and lower plates as in Figure 15. The total number of stud bolt connectors in the lower plate is one quarter of the section (XYZ) of the slab and is equal to $n_t/4$. For any yield line in one quarter of the section, the number of nut connections is $n_t/8$ and the tensile or compression force of the face plate along XY .yield line is as follows:

$$N_{t,Rd} = \frac{1}{8} n_t (P_R) \quad (12)$$

Therefore, total bending capacity on XY line is as follows:

$$M_{pl} = \frac{1}{8} n_t (P_R)(h_c + t) \quad (13)$$

And moment per unit width along the yield line is as follows:

$$m_{pl} = M_{pl} / l \quad (14)$$

If $l = L_s/(2\cos\theta)$, substituting the relation 14 in the relation 2, the load-carrying capacity of a SCS slab under concentrated load can be determined.

8- Comparison of the results of analytical relations with test results

Bending capacity of SCSB sandwich slabs under concentrated load is obtained from test results and is compared with the results of analytical method described in section 6. Partial factor is assumed to be γ_c=1.00. First, the shear capacity of stud bolt connectors is computed using the relation 1 and is presented in Table 7. Using the relation 2, the bending capacity of SCSB sandwich slabs is calculated and compared with test results in Table 8.

Table 7. Shear capacity of stud bolt connectors

Test sample	d (mm)	h_c (mm)	t (mm)	f_c (MPa)	A_s (mm^2)	h_c/d	P_R (kN)
SB8-1	8	80	6	38	50.27	10.00	30.10
SCSB8-2	8	100	6	38	50.27	12.50	33.35
SCSB8-3	8	150	6	38	50.27	18.75	40.19
SCSB10-1	10	80	6	38	78.54	10.00	42.44
SCSB10-2	10	100	6	38	78.54	12.50	47.02
SCSB10-3	10	150	6	38	78.54	18.75	56.67
SCSB12-1	12	80	6	38	113.10	10.00	56.19
SCSB12-2	12	100	6	38	113.10	12.50	62.27
SCSB12-3	12	150	6	38	113.10	18.75	75.03

Table 8. Comparison of bending capacity of SCSB slabs using analytical and test methods

Test sample	n_t	σ (Mpa)	P_R (kN)	M_{pl} (kN.m)	m_{pl} (kN)	F_p (kN)	$F_{p\text{-}exp}$ (kN)	$F_p / F_{p\text{-}exp}$
SCSB8-1	121	323	30.10	39.15	46.13	428.62	423	0.99
SCSB8-2	121	323	33.35	53.47	63.01	585.41	455	0.78
SCSB8-3	49	323	40.19	38.40	45.25	420.42	240	0.57
SCSB10-1	121	323	42.44	55.20	65.05	604.38	648	1.07
SCSB10-2	121	323	47.02	75.39	88.85	825.46	660	0.80
SCSB10-3	49	323	56.67	54.14	63.81	529.83	440	0.74
SCSB12-1	121	323	56.19	73.09	86.14	800.30	570	0.71
SCSB12-2	121	323	62.27	99.83	117.65	1093.04	600	0.55
SCSB12-3	49	323	75.03	71.69	84.49	785.00	750	0.96

Except SCSB10-1 sample, values of analytical relations are more than test results in all samples, showing that analytical relations are at the confidence level. The mean value of the ratio of test results to analytical results is 0.80 and standard deviation is 0.71. In cases such as SCSB8-3 and SCSB12-2, the ratio of the flexural strength of the test to the theory is considerably less than one. The main reason for this is that in calculating theoretical relationships it is assumed that the three-layer slabs work as a complete composite, but the investigation of the failure patterns of the experiments showed that in some samples, the layers were not complete composite.

9- Conclusions

In this article, nine test samples of SCSB slabs were prepared and load-displacement curves of the slab's center were extracted after concentrated loading at the center of the slab. The bending strength of the test was compared with the results of analytical relations. The following results were obtained from the works performed:

1. After concentrated loading at the center of SCSB slabs, failure modes observed from the tests included concrete failure, slip of lower plate, failure of stud bolts and buckling of steel face plates.
2. According to the load-displacement curves, it is observed that as the stud bolt diameter increases, more force is needed for a constant displacement, showing a direct relationship between stud bolt diameter and SCS slab strength. Also, samples' stiffness increased as the diameter increased.
3. Due to the increase in the concrete core thickness, the sample's stiffness and strength increased. The increase in the strength continues until the concrete reaches its ultimate strength.
4. Load-slip curves show that in slabs with a higher stud bolt diameter, the relative slip of the concrete core and the lower steel plate and the number of separated stud bolts decrease.
5. Comparing the curves of sandwich slabs with stud bolt connectors and those of slabs with ordinary concrete, it is concluded that the strength and ductility of SCSB sandwich slabs are more than ordinary slabs and their stiffness is lower.
6. Sandwich slabs with stud bolt connectors show more ductile behavior and better composite performance compared to sandwich slabs with J-hook connectors.
7. Comparing the results from analytical relations and test for the bending strength of SCSB slab, it is observed that the results are close to each other and analytical relations are at the confidence level. Analytical results can be employed to predict the bending strength of the sample.

References

[1] S. Solomon, D. Smith, A. Cusens, Flexural tests of steel-concrete-steel sandwiches, Magazine of Concrete Research, 28(94) (1976) 13-20.

[2] B. Burgan, F. Naji, Steel-concrete-steel sandwich construction, Journal of Constructional Steel Research, 46(1-3) (1998) 219.

[3] Y.-B. Leng, X.-B. Song, H.-L. Wang, Failure mechanism and shear strength of steel–concrete–steel sandwich deep beams, Journal of Constructional Steel Research, 106 (2015) 89-98.

[4] V. Thang, P. Marshall, N.A. Brake, F. Adam, Studded bond enhancement for steel-concrete-steel sandwich shells, Ocean Engineering, 124 (2016) 32-41.

[5] G.P. Zou, P.X. Xia, X.H. Shen, P. Wang, Investigation on the failure mechanism of steel-concrete steel composite beam, Steel and Composite Structures, 20(6) (2016) 1183-1191.

[6] Y. Leng, X. Song, Application of steel-concrete-steel sandwich deep beams into coupled shear walls, Advances in Structural Engineering, 22(1) (2019) 214-222.

[7] P. Marshall, A. Palmer, J. Liew, T. Wang, M. Thein, Bond enhancement for sandwich shell ice wall, International Conference and Exhibition on Performance of Ships and Structures in Ice, (2010).

[8] N. Foundoukos, M. Xie, J. Chapman, Fatigue tests on steel–concrete–steel sandwich components and beams, Journal of Constructional Steel Research, 63(7) (2007) 922-940.

[9] M. Xie, N. Foundoukos, J. Chapman, Static tests on steel–concrete–steel sandwich beams, Journal of Constructional Steel Research, 63(6) (2007) 735-750.

[10] X. Dai, J.R. Liew, Fatigue performance of lightweight steel–concrete–steel sandwich systems, Journal of Constructional Steel Research, 66(2) (2010) 256-276.

[11] W. Zuk, Prefabricated sandwich panels for bridge decks, Transportation Research Board Special Report, (148) (1974).

[12] T. Oduyemi, H. Wright, An experimental investigation into the behaviour of double-skin sandwich beams, Journal of Constructional Steel Research, 14(3) (1989) 197-220.

[13] T. Roberts, D. Edwards, R. Narayanan, Testing and analysis of steel-concrete-steel sandwich beams, Journal of Constructional Steel Research, 38(3) (1996) 257-279.

[14] T. Roberts, O. Dogan, Fatigue of welded stud shear connectors in steel–concrete–steel sandwich beams, Journal of Constructional Steel Research, 45(3) (1998) 301-320.

[15] O. Dogan, T. Roberts, Comparing experimental deformations of steel-concrete-steel sandwich beams with full and partial interaction theories, International Journal of Physical Sciences, 5(10) (2010) 1544-1557.

[16] O. Dogan, T. Roberts, Fatigue performance and stiffness variation of stud connectors in steel–concrete–steel sandwich systems, Journal of Constructional Steel Research, 70 (2012) 86-92.

[17] R. Narayanan, T.M. Roberts, F. Naji, Design guide for steel-concrete-steel sandwich construction, Steel Construction Institute, 1994.

[18] H. Bowerman, M. Gough, C. King, Bi-Steel design and construction guide, British Steel Ltd, Scunthorpe (London), (1999).

[19] H. Bowerman, J. Chapman, Bi-steel concrete steel sandwich construction, in: The fourth US Engineering Foundation conference on composite construction, June, 2000.

[20] H. Bowerman, N. Coyle, J. Chapman, An innovative steel/concrete construction system, Structural Engineer, 80(20) (2002) 33-38.

[21] M. Xie, J.C. Chapman, Static and fatigue tensile strength of friction-welded bar–plate connections embedded in concrete, Journal of Constructional Steel Research, 61(5) (2005) 651-673.

[22] M. Xie, N. Foundoukos, J. Chapman, Experimental and numerical investigation on the shear behaviour of friction-welded bar–plate connections embedded in concrete, Journal of Constructional Steel Research, 61(5) (2005) 625-649.

[23] J.R. Liew, K. Sohel, Lightweight steel–concrete–steel sandwich system with J-hook connectors, Engineering structures, 31(5) (2009) 1166-1178.

[24] J.R. Liew, K. Sohel, C. Koh, Impact tests on steel–concrete–steel sandwich beams with lightweight concrete core, Engineering Structures, 31(9) (2009) 2045-2059.

[25] K. Sohel, J.R. Liew, Steel–Concrete–Steel sandwich slabs with lightweight core—Static performance, Engineering Structures, 33(3) (2011) 981-992.

[26] J.-B. Yan, Ultimate strength behavior of steel–concrete–steel sandwich composite beams and shells, PhD thesis 2012, National University of Singapore, Singapore, 2012.

[27] J.-b. Yan, J.R. Liew, K. Sohel, M. Zhang, Push-out tests on J-hook connectors in steel–concrete–steel sandwich structure, Materials and structures, 47(10) (2014) 1693-1714.

[28] J.-B. Yan, J.R. Liew, M.-H. Zhang, J. Wang, Ultimate strength behavior of steel-concrete-steel sandwich beams with ultra-lightweight cement composite, Part 1: Experimental and analytical Study, Steel and Compsite Structures, 17(6) (2014) 907-927.

[29] J.-B. Yan, Finite element analysis on steel–concrete–steel sandwich beams, Materials and Structures, 48(6) (2015) 1645-1667.

[30] J.-B. Yan, J. Liew, M.-H. Zhang, Ultimate strength behavior of steel-concrete-steel sandwich beams with ultra-lightweight cement composite, Part 2: finite element analysis, Steel and Composite Structures, 18(4) (2015) 1001-1021.

[31] J.R. Liew, K.J.A.i.S.E. Sohel, Structural performance of steel-concrete-steel sandwich composite structures, 13(3) (2016) 453-470.

[32] J.R. Liew, J.-B. Yan, Z.-Y. Huang, Steel-concrete-steel sandwich composite structures-recent innovations, Journal of Constructional Steel Research, 130 (2017) 202-221.

[33] M. Yousefi, M. Ghalehnovi, Push-out test on the one end welded corrugated-strip connectors in steel-concrete-steel sandwich structure, Steel and Composite Structures, 24 (2017).

[34] M. Yousefi, M. Ghalehnovi, Finite element model for interlayer behavior of double skin steel-concrete-steel sandwich structure with corrugated-strip shear connectors, Steel and Composite Structures, 27 (2018).

[35] J.R. Liew, Innovative SCS system for marine and offshore applications, (2008).

[36] R. Soty, H. Shima, Formulation for maximum shear force on L-shape shear connector subjected to strut compressive force at splitting crack occurrence in steel-concrete composite structures, Procedia Engineering, 14 (2011) 2420-2428.

[37] M. Shariati, N.R. Sulong, M. Suhatril, A. Shariati, M.A. Khanouki, H. Sinaei, Behaviour of C-shaped angle shear connectors under monotonic and fully reversed cyclic loading: an experimental study, Materials & Design, 41 (2012) 67-73.

[38] M. Leekitwattana, S. Boyd, R. Shenoi, Evaluation of the transverse shear stiffness of a steel bi-directional corrugated-strip-core sandwich beam, Journal of Constructional Steel Research, 67(2) (2011) 248-254.

[39] M. Golmohammadi, M. Ghalehnovi, Testing and numerical modelling of Steel-Concrete-Steel with stud bolts connectors subject to push-out loading, Journal of Rehabilitation in Civil Engineering, 6 (2018).

[40] G. Rankin, A.J.P.o.t.I.o.C.E. Long, Predicting the punching strength of conventional slab-column specimens, 82(2) (1987) 327-346.

[41] K. Sohel, J.R.J.E.S. Liew, Steel–Concrete–Steel sandwich slabs with lightweight core—Static performance, 33(3) (2011) 981-992.

[42] Eurocode4, Design of Composite Steel and Concrete Structures. Part 1.1: General Rules and Rules for Buildings, BS EN 1994-1-1 :2004, 2004.

[43] B.S. Institution, Eurocode 2: Design of Concrete Structures: Part 1-1: General Rules and Rules for Buildings, British Standards Institution, 2004.

Please cite this article using:

M. Golmohammadi, M. Ghalehnovi, M. Yousefi, Experimental investigation of steel-concrete-steel slabs with stud bolt connectors subjected to punching loading, *AUT J. Civil Eng.*, 3(1) (2019) 93-106.

DOI: 10.22060/ajce.2018.14763.5496